









## RESEARCH ARTICLE

Cite this: *RSC Med. Chem.*, 2021, 12, 615

## Novel fluorinated ring-fused chlorins as promising PDT agents against melanoma and esophagus cancer†

Nelson A. M. Pereira, <sup>a</sup> Mafalda Laranjo, <sup>bcd</sup> Bruno F. O. Nascimento, <sup>a</sup> João C. S. Simões, <sup>ab</sup> João Pina, <sup>a</sup> Bruna D. P. Costa, <sup>ab</sup> Gonçalo Brites, <sup>b</sup> João Braz, <sup>ab</sup> J. Sérgio Seixas de Melo, <sup>a</sup> Marta Pineiro, <sup>a</sup> Maria Filomena Botelho <sup>bcd</sup> and Teresa M. V. D. Pinho e Melo <sup>★a</sup>

Investigation of novel 4,5,6,7-tetrahydropyrazolo[1,5-a]pyridine-fused chlorins, derived from 5,10,15,20-tetrakis(pentafluorophenyl)porphyrin, as PDT agents against melanoma and esophagus cancer is disclosed. Diol and diester fluorinated ring-fused chlorins, including derivatives with 2-(2-hydroxyethoxy)ethanamino groups at the phenyl rings, were obtained *via* a two-step methodology, combining  $S_NAr$  and  $[8\pi + 2\pi]$  cycloaddition reactions. The short-chain PEG groups at the *para*-position of the phenyl rings together with the diol moiety at the fused pyrazole ring promote a red-shift of the Soret band, a decrease of the fluorescence quantum yield and an increase of the singlet oxygen formation quantum yield, improving the photophysical characteristics required to act as a photosensitizer. Introduction of these hydrophilic groups also improves the incorporation of the sensitizers by the cells reaching cellular uptake values of nearly 50% of the initial dose. The rational design led to a photosensitizer with impressive  $IC_{50}$  values, 13 and 27 nM against human melanoma and esophageal carcinoma cell lines, respectively.

Received 28th December 2020,  
Accepted 22nd March 2021

DOI: 10.1039/d0md00433b

rsc.li/medchem

## Introduction

The combination of oxygen, light and a photosensitizing agent with the goal of destroying abnormal cells in cancer and other diseases, including pathogenic infections, is the basic principle of photodynamic therapy (PDT).<sup>1–3</sup> Briefly, the activation of the photosensitizer (PS) upon light irradiation leads to the formation of so-called reactive oxygen species (ROS) from molecular oxygen *via* energy and/or electron transfer processes.<sup>4</sup> These ROS promote a significant cytotoxic effect, causing damage to cellular organelles, harming associated tissue vasculature, and triggering inflammation and subsequent immune response. As these processes take place within the close environment of the light-absorbing sensitizer, the selective accumulation of the PS in tumor tissues and the utilization of suitable excitation light yields a

generalized decrease of off-target damage. Consequently, side-effects are diminished when compared to systemic cancer chemotherapy and radiotherapy treatments.<sup>5,6</sup> Therefore, it comes as no surprise that PDT is being increasingly regarded as a fitting therapeutic strategy in the management of cancers, either alone or in combination arrangements, along with radio, chemo and immunotherapies.<sup>7–10</sup>

Esophageal cancer is the 7th most ordinarily occurring cancer worldwide, with nearly 604 000 new cases and about 537 000 deaths being estimated for 2020, according to the most recent data of the Global Cancer Observatory at the International Agency for Research on Cancer.<sup>11,12</sup> Between 40 and 50% of patients with esophageal cancer are deemed surgically unresectable and, of those resected, only around 15 to 20% have a chance for cure or long-time survival.<sup>13,14</sup> Therefore, the usual treatment for the majority of cases is simple palliation of symptoms, *i.e.* the relief of dysphagia. More recently, endoscopic photo-irradiation was found to relieve malignant obstruction of the esophagus, which led to PDT using photofrin and diode laser irradiation as an approved treatment for superficial esophageal cancer.<sup>14</sup> While endoscopic submucosal dissection (ESD) is currently a more popular management approach for esophageal cancer, there is plentiful evidence to support PDT as an effective and alternative clinical treatment modality and/or recovery treatment for local failure after chemoradiotherapy.<sup>15,16</sup>

<sup>a</sup> Coimbra Chemistry Centre (CQC) and Department of Chemistry, University of Coimbra, 3004-535 Coimbra, Portugal. E-mail: tmelo@ci.uc.pt

<sup>b</sup> Institute of Biophysics and Institute for Clinical and Biomedical Research (iCBR), Area of Environment Genetics and Oncobiology (CIMAGO), Faculty of Medicine, University of Coimbra, 3000-548 Coimbra, Portugal

<sup>c</sup> Center for Innovative Biomedicine and Biotechnology (CIBB), University of Coimbra, 3000-548 Coimbra, Portugal

<sup>d</sup> Clinical and Academic Centre of Coimbra, 3000-548 Coimbra, Portugal

† Electronic supplementary information (ESI) available. See DOI: 10.1039/d0md00433b

Another mounting concern in terms of global health is skin cancer. Both melanoma and non-melanoma skin cancers are among the most common malignancies in Caucasians, with increasing incidence over the past few years. There are nearly 302 000 new cases and around 64 000 deaths being projected for 2020 as a result of malignant melanoma.<sup>11,12</sup> Albeit being one of the least common forms of skin cancer, it is also one of the deadliest types because of its potential to spread to other parts of the body. Summing up the rising incidence rates of malignant melanoma with its growing resistance to conventional chemotherapy and radiotherapy, an effective and alternative therapeutic strategy, such as photodynamic therapy, can be easily perceived as an urgent need. Although PDT has been successfully applied in the treatment of skin conditions and malignancies,<sup>17</sup> its use in malignant melanoma can be compromised due to the natural resistance mechanism of some melanoma tumor cells. Particularly, high melanin levels in pigmented tumors can stimulate an antioxidant effect, due to optical interference *via* competition with the photosensitizer for the absorption of light.<sup>18</sup> Being an aggressive form of skin cancer with an unfavorable prognosis, particularly in advanced stages, the search for new and more proficient PSs able to overcome the resistance of malignant melanoma to photodynamic therapy is highly necessary.<sup>19</sup>

Tetrapyrrolic macrocycles constitute a class of naturally-occurring heteroaromatic molecules with undeniable biological importance.<sup>20</sup> Due to their chemical and photophysical properties, such as effective light absorption and emission within the phototherapeutic window (600–850 nm), great ROS generation capabilities, customarily low toxicity *in vivo*, and commonly easy structural derivatization, porphyrins and related compounds are broadly recognized as worthy photosensitizers for cancer imaging and therapy.<sup>5,6,21,22</sup> A new class of free base ring-fused chlorins (dihydroporphyrins) has been developed by us *via* a  $[8\pi + 2\pi]$  cycloaddition methodology,<sup>23,24</sup> some of them being successfully evaluated as potent PDT agents against different tumor cell lines.<sup>25–27</sup> A similar strategy was also applied in our group to obtain platinum(II) ring-fused chlorins with improved near-infrared (NIR) luminescence, ratiometric molecular oxygen sensing, and photodynamic action features for cancer theranostic applications.<sup>28,29</sup> More recently, the most efficient ring-fused chlorins were studied *in vivo*, showing an impressive ability as photosensitizers for detection and treatment of malignant tumors.<sup>27,29</sup> Although a powerful photodynamic effect has been established for some of these derivatives, both *in vitro* and *in vivo*, we decided to widen the range of our ongoing studies in order to encompass ring-fused *meso*-substituted chlorin derivatives with pentafluorophenyl groups. This would be a strategy to allow further functionalization since it is known that 5,10,15,20-tetrakis(pentafluorophenyl)porphyrin reacts with a variety of nucleophiles *via* nucleophilic aromatic substitution ( $S_NAr$ ) reactions.<sup>30</sup> On the other hand, perfluoroporphyrins are reported to be particularly stable

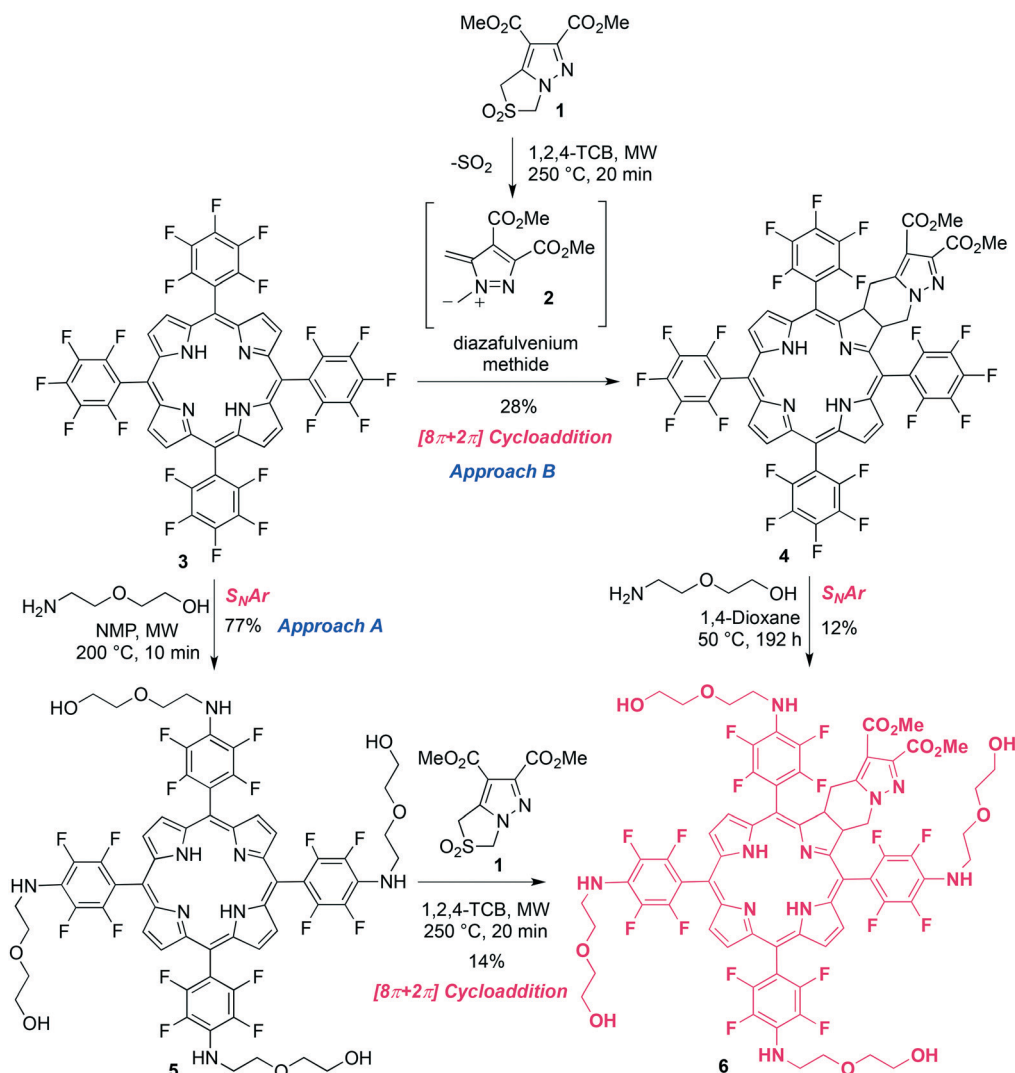
against oxidation (increased photostability)<sup>31,32</sup> and efficient singlet oxygen generators.<sup>33</sup>

Bearing in mind that the inherent features of PSs such as photophysics, hydrophilic/lipophilic nature, shape, size and overall structure are crucial to localize and buildup PSs in several cellular organelles,<sup>34,35</sup> the amphiphilic character of photosensitizers was modulated by functional group interconversion and specific peripheral substitutions. The reduction of methyl ester substituents, located at the exocyclic ring, into hydroxymethyl groups was one of the design structural modulations with the purpose of increasing the polarity of the resulting ring-fused chlorins. The second structural modulation was the incorporation of poly(ethylene glycol) (PEG) moieties, a well-known methodology applied in drug design to obtain compounds with the ideal properties to be employed in biological media and improve cell permeability.<sup>36</sup> Synthetic details, structural and photophysical characterization, *in vitro* photocytotoxicity, cell viability and uptake assessment of these novel PEGylated and/or fluorinated 4,5,6,7-tetrahydropyrazolo[1,5-*a*]pyridine-fused chlorin products, in both A375 skin malignant melanoma and OE19 esophageal adenocarcinoma cell lines, are reported herein.

## Results and discussion

### Synthesis

We have designed and developed a new class of ring-fused free base and Pt(II) chlorins that were found to be excellent candidates for cancer PDT.<sup>23–28</sup> Furthermore, our studies demonstrated that the hydrophilicity of these chlorins is crucial to ensure high photocytotoxicity in tumor cells.<sup>25–28</sup> From a chemical standpoint, the 4,5,6,7-tetrahydropyrazolo[1,5-*a*]pyridine-fused chlorin structure bearing *meso*-substituted pentafluorophenyl moieties can be viewed as a novel and versatile template for further derivatization. Much like its broadly known 5,10,15,20-tetrakis(pentafluorophenyl)porphyrin 3 (TPPF<sub>20</sub>) analogue, a simple nucleophilic aromatic substitution process with a range of suitable nucleophiles provides general access to functionalized derivatives comprising electron-donating substituents at the *para* positions of the phenyl rings, with this reaction being extremely selective and frequently high yielding.<sup>30,37,38</sup> Based on this, we decided to synthesize novel PEGylated derivatives of this type of ring-fused chlorins in order to get compounds with better molecular features to be used as photosensitizers. Two different approaches were carried out to obtain the target ring-fused chlorin 6 (Scheme 1). The first synthetic route (approach A) started with the PEGylation of 5,10,15,20-tetrakis(pentafluorophenyl)porphyrin 3, adapting a procedure reported by Drain and collaborators<sup>30</sup> for the nucleophilic aromatic substitution of the *para*-fluorine atoms of TPPF<sub>20</sub> by primary amines. Thus, the  $S_NAr$  reaction of porphyrin 3 with 10 equivalents of 2-(2-aminoethoxy)ethanol (amine-PEG) in *N*-methyl-2-pyrrolidone (NMP), under microwave irradiation (MW) at 200 °C for 2



**Scheme 1** Schematic routes to PEGylated chlorin **6**.

minutes, afforded the tetrasubstituted porphyrin **5** in only 9% yield after isolation (Table 1, entry 1). A better result was obtained when the reaction time was increased to 5 minutes, giving the desired product in 42% yield (entry 2). Very minor improvements were observed under similar conditions but using a larger excess of amine-PEG (20 equivalents) or by carrying out the reaction at a lower temperature (70 °C) for a longer period of time (18 minutes) (entries 3 and 4,

**Table 1** Optimization of the PEGylation of 5,10,15,20-tetrakis(pentafluorophenyl)porphyrin with 2-(2-aminoethoxy)ethanol carried out in NMP

Entry	Equiv. amine-PEG	Reaction conditions	Yield (%)
1	10	MW, 200 °C, 2 min	9
2	10	MW, 200 °C, 5 min	42
3	20	MW, 200 °C, 5 min	45
4	10	MW, 70 °C, 18 min	48
5	10	MW, 200 °C, 10 min	77
6	10	200 °C, 3 h	68

respectively). The best microwave-promoted reaction conditions were achieved by performing the reaction at 200 °C for 10 minutes using 10 equivalents of 2-(2-aminoethoxy)ethanol (entry 5), with porphyrin **5** being isolated in 77% yield. Changing to a conventional heating setting allowed a 10-fold scale-up and after 3 hours at 200 °C and similar work-up, the target porphyrin was obtained in 68% yield (entry 6). The  $\text{S}_{\text{N}}\text{Ar}$  reaction proved to be very selective occurring, as expected, at the *para* positions of the *meso*-pentafluorophenyl groups of porphyrin **3**. This can be clearly confirmed by the  $^{19}\text{F}$  NMR spectrum of porphyrin **5** showing only two doublets at  $-143$  and  $-160$  ppm, both with a 19.0 Hz coupling constant, corresponding to 8 *ortho*- and 8 *meta*-fluorine atoms. On the other hand, peaks characteristic of the *para*-fluorine atoms at *ca.*  $-150$  ppm of pentafluorophenyl groups are absent.<sup>39</sup> Moreover, in the  $^1\text{H}$  NMR spectrum, signals corresponding to the short-chained PEG hydrogen atoms (4 NH and 16  $\text{CH}_2$ ) appear at 4.74 ppm and 3.6–3.8 ppm, respectively (see Fig. S1†).

In order to achieve the desired PEGylated and fluorinated chlorin **6**, a  $[8\pi + 2\pi]$  cycloaddition reaction of porphyrin **5** with diazafulvenium methide **2**, generated *in situ* by thermal extrusion of  $\text{SO}_2$  from 2,2-dioxo-1*H*,3*H*-pyrazolo[1,5-*c*]thiazole **1**,<sup>40,41</sup> was carried out as described before for other ring-fused chlorin derivatives (Scheme 1, approach A).<sup>23,24</sup> Performing the reaction under microwave irradiation at 250 °C for 20 min, using 1,2,4-trichlorobenzene (1,2,4-TCB) as a solvent, chlorin **6** was obtained in 14% yield (Table 2, entry 1). An excess of porphyrin (2 equivalents) was used in order to prevent the formation of the corresponding bacteriochlorin *via* bis-cycloaddition of diazafulvenium methide **2** to porphyrin **5**. The  $^{19}\text{F}$  NMR spectrum of chlorin **6** is a bit more complex than the one of related porphyrin **5**, given that the introduction of the exocyclic fused-ring leads to structural asymmetry (see Fig. S3†). Nonetheless, it still presents signals within the ranges  $-138$  to  $-140$  ppm and  $-158$  to  $-160$  ppm, again typical of fluorine atoms at the *ortho* and *meta* positions of the *meso*-pentafluorophenyl groups, respectively, and no signals expected for *para*-fluorine atoms.<sup>39</sup> Switching to conventional heating allowed a 3-fold scale-up of the  $[8\pi + 2\pi]$  cycloaddition reaction. The reaction of porphyrin **5** with an equimolar and two equivalents of sulfone **1**, at 250 °C for 3 hours, afforded chlorin **6** in similar yields as determined by  $^1\text{H}$  NMR spectroscopy, 47% and 46%, respectively (Table 2, entries 2 and 3). Despite the better yields achieved under conventional heating, a mixture of the target chlorin and starting porphyrin, which we were unable to separate, was obtained. Therefore, the MW-induced reaction was found to be the best synthetic approach to prepare pure chlorin **6**. Nevertheless, we found that when derivative **7** was the target (Scheme 2), starting from the mixture proved to be a better option due to the possibility of working on a larger scale. Further details are described below.

An alternative strategy to obtain PEGylated compound **6** was pursued, which consisted of the synthesis of chlorin **4** followed by  $\text{S}_{\text{N}}\text{Ar}$  PEGylation (Scheme 1, approach B). The reaction between TPPF<sub>20</sub> and sulfone **1** (molar ratio of 2:1), upon microwave irradiation at 250 °C for 20 minutes, provided the new ring-fused 5,10,15,20-tetrakis(pentafluorophenyl)chlorin **4** in 24% yield. Performing the reaction under the same stoichiometric conditions, but under conventional heating for 3 hours at 250 °C, was also tested.

**Table 2** Optimization of the  $[8\pi + 2\pi]$  cycloaddition reaction of PEGylated porphyrin **5** with diazafulvenium methide **2** carried out in 1,2,4-TCB

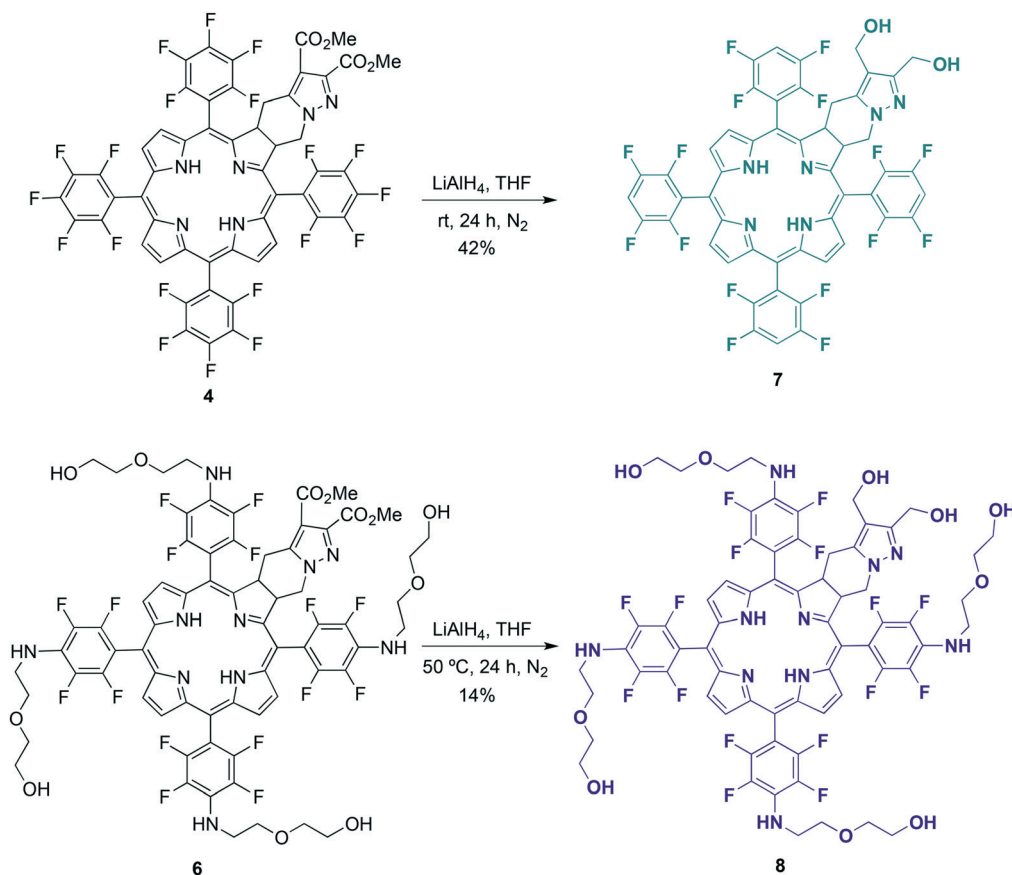
Entry	Equiv. porphyrin <b>5</b>	Reaction conditions	Yield (%)
1	2	MW, 250 °C, 20 min	14
2	1	250 °C, 3 h	47 <sup>a</sup>
3	0.5	250 °C, 3 h	46 <sup>a</sup>

<sup>a</sup> Yield of chlorin **6** contaminated with the starting porphyrin **5**, determined by  $^1\text{H}$  NMR from the mixture with a chlorin/porphyrin molar ratio of 2/1.

Although this procedure led to a slight improvement, with a 28% yield being attained, the MW method was preferred due to the considerably shorter reaction time. Then, we tried to PEGylate chlorin **4** under microwave irradiation under similar conditions used in the synthesis of porphyrin **5** (see Table 1). After several attempts, monitoring the reaction progress by UV-vis spectroscopy, we verified that the formed chlorin **6** partially degrades to its oxidized forms that we were unable to separate. Therefore, we decided to perform the reaction under milder conditions by lowering the temperature. Thus, carrying out the reaction under conventional heating at 50 °C, in 1,4-dioxane, for 192 hours, tetra-PEGylated chlorin **6** was obtained in 12% yield (Scheme 1, approach B). Hence, we have shown that chlorin **6** could be obtained *via* both synthetic routes. Nevertheless, the overall process through approach A is significantly faster and eco-friendlier and, therefore, more advantageous.

The reduction of the methyl ester substituents of chlorin **4** to their corresponding hydroxymethyl groups was also carried out (Scheme 2). Previously, we have demonstrated that this structural modification led to a considerable improvement in the PDT effectiveness of this type of photosensitizer, which is related to a higher cellular uptake of the hydroxymethyl derivatives.<sup>25–29</sup> The reduction was performed by reacting dimethyl ester chlorin **4** with an excess of lithium aluminum hydride (12 equivalents) in tetrahydrofuran (THF), at room temperature and under an inert  $\text{N}_2$  atmosphere, for 24 hours. After product isolation and  $^1\text{H}$  NMR analysis, we observed that not only the reduction had occurred, as could be confirmed by the replacement of two singlets corresponding to the methyl esters of chlorin **4** (nearly 3.8 and 4 ppm, see Fig. S2†) by two other singlets assigned to the two methylene groups of the hydroxymethyl substituents of chlorin **7** (around 4.4 and 4.6 ppm, see Fig. S4†) but, somewhat unexpectedly, the complete dehalogenation of the *para*-fluorine atoms on the aryl groups also took place. The dehalogenation could easily be confirmed by the presence of a multiplet at around 7.5 ppm corresponding to the aromatic protons of the four 2,3,5,6-tetrafluorophenyl groups in the  $^1\text{H}$  NMR spectrum of chlorin **7**, as well as by the significant changes regarding chemical shifts and multiplicities of the  $^{19}\text{F}$  NMR signals when compared to the spectroscopic information of the chlorin **4** starting material. These include the disappearance of the above-mentioned typical peaks of the *para*-fluorine atoms at *ca.*  $-150$  ppm.<sup>39</sup> The signals related to the *ortho*- and *meta*-fluorine atoms are observed between  $-135$  and  $-139$  ppm (see Fig. S2 and S4†). The reduction of aryl halides with lithium aluminum hydride is well known<sup>42–44</sup> and reductive dehalogenation of aryl fluorides under mild conditions was also demonstrated by Hendrix *et al.*<sup>43</sup> The new dihydroxymethyl chlorin **7** was thus obtained in 42% yield.

The preparation of chlorin **8** followed the same  $\text{LiAlH}_4$ -promoted reduction methodology described above for chlorin **7** (Scheme 2). As referred before, the synthesis of chlorin **6** under conventional heating can be carried out on a larger



Scheme 2 Synthesis of dihydroxymethyl chlorins **7** and **8**.

scale despite not being isolated in a pure form as *via* the MW-assisted protocol (Table 2). On the other hand, the reduction of the methyl ester substituents of the exocyclic chlorin scaffold to their corresponding hydroxymethyl groups would lead to a much more polar compound than porphyrin **5** contaminant and, hence, easier to separate after suitable chromatographic work-up. In this context, we decided to perform the reduction reaction to achieve **8** starting with the mixture containing chlorin **6** and TPPF<sub>20</sub>. The reaction with an excess of lithium aluminum hydride in THF, under a saturated N<sub>2</sub> atmosphere at 50 °C for 24 hours, led to the target chlorin **8** in 14% yield after isolation. In the <sup>9</sup>F NMR spectrum, signals corresponding to the *ortho*- (between -141 and -145 ppm) and *meta*-fluorine atoms, from -160 to -162 ppm (see Fig. S5<sup>†</sup>), clearly demonstrate that there was no unforeseen reductive dehalogenation process.

### Photophysical studies

The absorption and fluorescence emission spectra of chlorins **4** and **6–8** in dimethylsulfoxide (DMSO) solution at room temperature are presented in Fig. 1. The spectra show the characteristic absorption features of the chlorin macrocycle, with a strong Soret band with a maximum between 406 and 424 nm and a more pronounced Q band at ~653 nm, and also typical emission maxima at ~658 nm. Substitution of

the fluorine atoms at the *para* positions of the *meso*-aryl rings by short-chained PEG moieties (**6** and **8**) red-shifts by ~17 nm the absorption maxima of the Soret band, when compared to the non-PEGylated derivatives **4** and **7** (Table 3). Fluorescence lifetimes ( $\tau_F$ ) for all chlorin derivatives, collected with excitation at 373 nm in DMSO solution, were found to

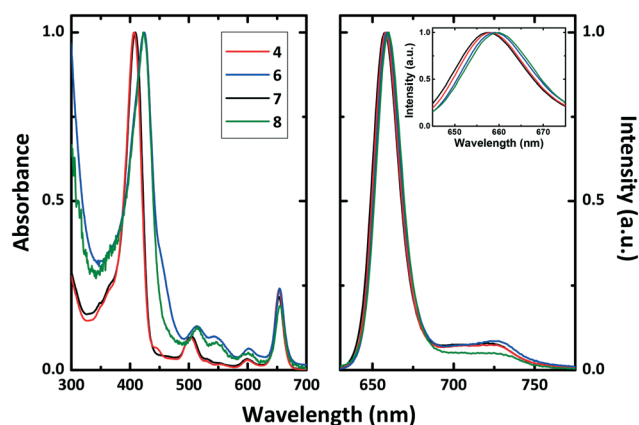


Fig. 1 Room temperature absorption (left hand panel) and fluorescence emission (right hand panel) spectra of chlorins **4** and **6–8** in DMSO solution. The inset in the emission spectra is a magnification of the Soret band, showing the shift with the substitution. See text for more details.

**Table 3** Spectroscopic (absorption, fluorescence and triplet absorption maxima) and photophysical data (including fluorescence ( $\phi_F$ ), internal conversion ( $\phi_{IC}$ ) and singlet oxygen sensitization ( $\phi_\Delta$ ) quantum yields, along with fluorescence lifetimes ( $\tau_F$ ), triplet lifetimes ( $\tau_T$ ) and rate constants,  $k_F$ ,  $k_{IC}$  and  $k_{ISC}$ ) for chlorins **4** and **6–8** in DMSO solution at 293 K

Chlorin	$\lambda_{\max}^{\text{Abs}}$ (nm)	$\lambda_{\max}^{\text{Fluo}}$ (nm)	$\lambda_{\max}^{T_1-T_n}$ (nm)	$\phi_F$	$\phi_{IC}^a$	$\phi_\Delta$	$\tau_F$ (ns)	$\tau_T$ ( $\mu$ s)	$k_F$ ( $\text{ns}^{-1}$ )	$k_{NR}^b$ ( $\text{ns}^{-1}$ )	$k_{ISC}^a$ ( $\text{ns}^{-1}$ )	$k_{IC}^a$ ( $\text{ns}^{-1}$ )
<b>4</b>	406, 653	658, 722	460	0.39	0.21	0.40	7.0	68	0.056	0.087	0.057	0.030
<b>6</b>	424, 654	659, 725	495	0.24	0.45	0.31	7.2	35	0.033	0.105	0.043	0.062
<b>7</b>	408, 653	657, 722	460	0.41	0.27	0.32	7.0	46	0.059	0.085	0.046	0.039
<b>8</b>	424, 654	659, 725	495	0.28	0.27	0.45	7.3	50	0.038	0.098	0.061	0.037

<sup>a</sup> Assuming  $\phi_T \sim \phi_\Delta$  and  $\phi_{IC} = 1 - \phi_F - \phi_T$ . <sup>b</sup>  $k_{NR} = (1 - \phi_F)/\tau_F$ .<sup>53</sup>

be well fitted with a single exponential decay law. Similar  $\tau_F$  were obtained for the investigated compounds, with values  $\sim 7$  ns (Table 3), in agreement with the data reported for a 5,10,15,20-tetrakis(pentafluorophenyl)chlorin bearing a *N*-benzylisoazolidine ring ( $\tau_F = 7.3$  ns).<sup>45</sup>

Triplet–triplet transient absorption spectra of deaerated solutions of the chlorin PSs were collected at different times after laser flash photolysis with excitation at 355 nm (see Fig. S6†). Similar transient triplet–triplet absorption spectra and triplet lifetimes ( $\tau_T = 35$ –68  $\mu$ s) were found (Table 3). In general, the triplet–singlet difference absorption spectra present positive broad transient absorption bands in the 300–550 nm range, attributed to the triplet–triplet absorption of the chlorins, together with negative transient absorption bands that are in agreement with the spectroscopic features presented in Fig. 1, which are attributed to the ground state absorption of the chlorins' Soret band. The triplet nature of transient absorption signals is supported by their quenching by oxygen in air-saturated solutions, which follows pseudo first order kinetics. Significant is that, in agreement with the behaviour found in the ground state absorption, the replacement of the *para*-fluorine atoms at the *meso*-substituted aryl rings by short-chained PEG groups red-shifts the triplet–triplet absorption maxima by  $\sim 35$  nm.

To evaluate the potential of our novel chlorin derivatives as PDT agents, singlet oxygen sensitization quantum yields ( $\phi_\Delta$ ) were obtained by direct measurement of the characteristic phosphorescence emission of  $^1\text{O}_2$ , following photolysis of aerated DMSO solutions of the compounds at  $T = 293$  K (Table 3). The  $\phi_\Delta$  values were determined using a comparative method, utilizing *meso*-tetraphenylporphyrin (TPP) in toluene as a reference photosensitizer, by plotting the initial phosphorescence intensity (at 1270 nm) as a function of the laser dose and comparing the slope with that obtained for the reference compound (Fig. S7†). Singlet oxygen formation quantum yields in the 0.31–0.45 range were obtained for the investigated chlorins (Table 3). Comparison with the parent non-fluorinated diphenylchlorins previously reported<sup>26</sup> shows that: (i) the  $\phi_\Delta$  value found for dihydroxymethyl-substituted chlorin **7** ( $\phi_\Delta = 0.32$ ) is in agreement with that found for the dihydroxymethyl-bearing diphenylchlorin ( $\phi_\Delta = 0.27$ ); (ii) regarding the dimethyl ester-substituted chlorin **4**, introduction of the fluorine atoms decreases the singlet oxygen production efficiency ( $\phi_\Delta = 0.40$ )

when compared to the non-fluorinated diester diphenylchlorin derivative ( $\phi_\Delta = 0.66$ ). Additionally, considering that in general the singlet oxygen quantum yields cannot be higher than the intersystem crossing (triplet formation) quantum yields ( $\phi_\Delta \leq \phi_T$ ), and assuming efficient triplet energy transfer from the long-lived triplet state of the fluorinated chlorins to the ground-state triplet molecular oxygen, *i.e.*  $S_\Delta = \phi_\Delta/\phi_T = 1$ , the obtained  $\phi_\Delta$  values can be considered a good estimate of the triplet formation quantum yields.

Table 3 summarizes the relevant photophysical parameters (quantum yields, lifetimes and rate constants) obtained for the studied chlorin derivatives in DMSO solution. The fluorescence quantum yields values ( $\phi_F$ ) show that the introduction of short-chained PEG moieties decreases the efficiency of the excited-state radiative decay channel ( $\phi_F = 0.39$  and 0.41 for chlorins **4** and **7**, respectively, *vs.*  $\phi_F = 0.24$  and 0.28 for chlorins **6** and **8**). From the overall photophysical parameters in Table 3, we can conclude that, in general, the radiationless deactivation processes are the main excited state deactivation channels, contributing more than 60% ( $\phi_{IC} + \phi_T$ ) to the excited state deactivation of these ring-fused chlorins. However, in contrast with the behaviour found for chlorins **4**, **7** and **8** (where the radiationless ISC channel is predominant), for PEGylated chlorin **6** the internal conversion decay channel is now the main radiationless decay process (with  $\phi_{IC} \sim 0.45$  *vs.* 0.21–0.27 for the non-PEGylated chlorins). When the dimethyl ester- and dihydroxymethyl-substituted chlorins and their halogen-free 5,15-diphenylchlorin derivatives<sup>26</sup> are compared, a  $\sim 1$ -fold increase in the fluorescence quantum yield was observed with the introduction of the fluorine atoms. This result is in line with the small or null heavy atom effect observed with the pentafluorophenyl substitution at the porphyrin macrocycle.<sup>33,46</sup> Table 3 also shows that the excited state deactivation rate constants ( $k_F$ ,  $k_{IC}$  and  $k_{ISC}$ ) are all in the same order of magnitude ( $\sim 10^{-11}$   $\text{s}^{-1}$ ) thus showing that all the decay processes are competitive with the deactivation of  $S_1$ .

## Cell biology

To evaluate the activity of these new compounds as photosensitizers for photodynamic therapy, the human

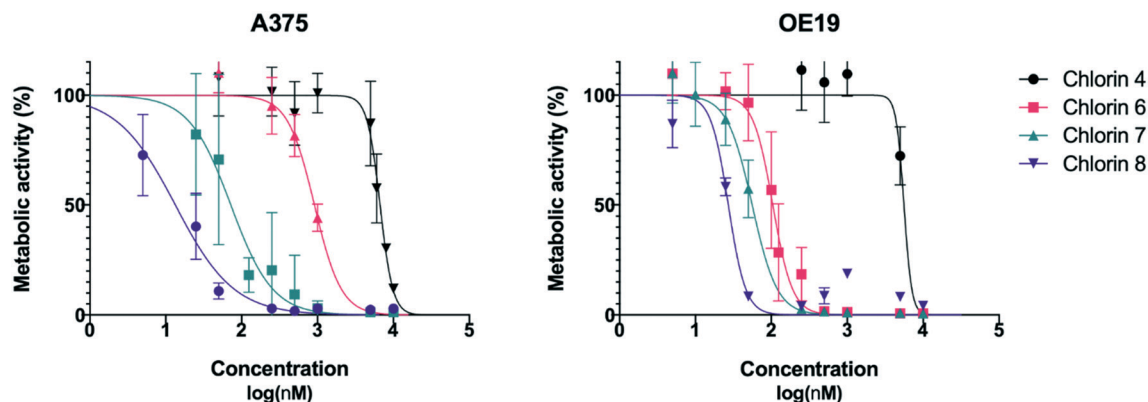


Fig. 2 Dose–response curves of A375 skin malignant melanoma cells (left) and OE19 esophageal adenocarcinoma cells (right). Analysis performed 24 hours after PDT using chlorins 4, 6, 7 and 8 with an energy of 10 J. Data points represent the mean  $\pm$  SD.

melanoma A375 and esophageal carcinoma OE19 cell lines were exposed to increasing concentrations of chlorins 4 and 6–8 and then subjected to irradiation with filtered light ( $\text{cut}_{\text{off}} < 560 \text{ nm}$ ). Control samples to evaluate the cytotoxicity of the PSs and from irradiation alone were also performed. The sigmoid dose–response curves shown in Fig. 2 were adjusted from the experimental results, allowing the  $\text{IC}_{50}$  values and the respective 95% confidence intervals to be determined, which are presented in Table 4.

Upon light irradiation, chlorins 4 and 6–8 showed dose dependent toxicity against the human melanoma and esophageal carcinoma cells. Not surprisingly, chlorin 4 revealed limited photodynamic activity with  $\text{IC}_{50}$  values in the micromolar range in both cell lines. Similar behavior was previously observed with other 4,5,6,7-tetrahydropyrazolo[1,5-*a*]pyridine-fused chlorins bearing diester moieties in the fused ring.<sup>25,28,29</sup> The strong hydrophobic character should be the main factor for the low activity.

It has been previously demonstrated that the reduction of diester groups to dihydroxymethyl groups in several 4,5,6,7-tetrahydropyrazolo[1,5-*a*]pyridine-fused chlorins contributes to a higher photodynamic reaction.<sup>25–29</sup> This phototoxicity improvement was also observed, changing from fluorinated chlorin 4 to 7 (Table 4). Unlike chlorin 4, the dihydroxymethyl derivative 7 showed a very interesting

activity against both cell lines studied [ $\text{IC}_{50}$  (A375) = 72 nM;  $\text{IC}_{50}$  (OE19) = 56 nM].

As mentioned above, coupling hydrophobic compounds to PEG moieties is an attractive option for improving their hydrophilicity. This strategy was also explored to achieve a sensitizer with more appropriate features, introduction of PEG moieties in the aryl substituents of chlorin 4 leading to chlorin 6. Undoubtedly, the biological activity of chlorin 6 increased significantly, with greater relevance in the esophageal carcinoma cells with an  $\text{IC}_{50}$  value of 105 nM (Table 4).

The two structural modulations, introduction of dihydroxymethyl groups or introduction of PEG moieties, led to new and particularly interesting fluorinated sensitizers, chlorins 6 and 7, with PDT activity in the nanomolar range. These promising results justified the study as a PDT agent of chlorin 8, which incorporates the two referred structural features. Hence, PDT assays were performed in A375 and OE19 cells. Remarkably, chlorin 8 proved to be the most active PS of this series. This compound exhibited impressive  $\text{IC}_{50}$  values, values as low as 13 and 27 nM against the human melanoma and esophageal carcinoma cell lines, respectively (Table 4).

Another characteristic of these compounds, which is extremely important considering their application as sensitizers for PDT, is the lack of toxicity in the absence of light. The dark experiments revealed that no effect was seen up to the highest concentration tested of 10  $\mu\text{M}$ , as shown in Table 4.

The differences observed in the PDT activity of the most relevant chlorins 6–8 can be rationalized based on two important properties, the ability to produce ROS, namely singlet oxygen, and the ability to reach intracellular targets. Regarding the production of the cytotoxic oxygen species, chlorins 6 and 7 exhibit similar singlet oxygen sensitization quantum yields in solution ( $\phi_{\Delta} \approx 0.30$ ), as can be verified in the photophysical data shown in Table 3. Interestingly, chlorin 8 presented the highest singlet oxygen yield ( $\phi_{\Delta} = 0.45$ ). The second crucial property for PDT efficiency is the incorporation of the sensitizers by the cells. Therefore, uptake studies were performed in both cell lines, as represented in Fig. 3. In fact, the highest photodynamic

Table 4 Photocytotoxicity:  $\text{IC}_{50}$  and respective  $\text{CI}_{95}$  values of chlorins 4 and 6–8 in A375 skin malignant melanoma and OE19 esophageal adenocarcinoma cells. Analysis performed 24 hours after PDT with an energy of 10 J. Cytotoxicity was determined omitting the irradiation step. Values were determined by dose–response sigmoidal fitting ( $r^2 > 0.85$ )

Chlorin	Photocytotoxicity (nM)				Cytotoxicity ( $\mu\text{M}$ )	
	A375		OE19		A375	OE19
	$\text{IC}_{50}$	$\text{CI}_{95}$	$\text{IC}_{50}$	$\text{CI}_{95}$	$\text{IC}_{50}$	$\text{IC}_{50}$
4	6681	[6179; 7241]	5606	[4220; nd]	>10	>10
6	913	[749; 1145]	105	[91; 122]	>10	>10
7	72	[54; 97]	56	[49; 68]	>10	>10
8	13	[9; 18]	27	[13; 37]	>10	>10

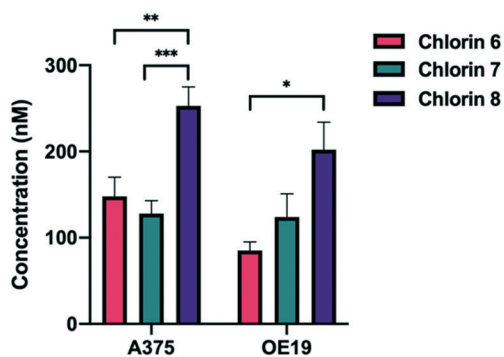


**Fig. 3** Uptake of chlorins 6, 7 and 8 by A375 skin malignant melanoma and OE19 esophageal adenocarcinoma cells. The cells were incubated for 24 hours with 500 nM of each photosensitizer. Data points represent the mean  $\pm$  SE.

activity of chlorin 8 may be related to the uptake of this compound. In the human melanoma A375 cells, nearly 50% ( $254 \pm 22$  nM) of compound 8 entered the cells, significantly higher than chlorin 6 ( $148 \pm 22$  nM;  $p = 0.004$ ) and chlorin 7 ( $128 \pm 15$  nM;  $p = 0.0006$ ). Similarly, in the human esophageal carcinoma OE19 cells, a higher uptake of chlorin 8 was found, with a concentration of  $202 \pm 32$  nM. Hence, these two combined abilities of chlorin 8 lead to the enhancement of intracellular ROS production resulting in its superior PDT efficacy.

## Conclusions

Fluorinated and PEGylated ring-fused chlorins, bearing methyl ester substituents, have been synthesized by exploring  $[8\pi + 2\pi]$  cycloaddition of perfluoroporphyrins with the diazafulvenium methide derived from dimethyl 2,2-dioxo-1*H*,3*H*-pyrazolo[1,5-*c*]thiazole-6,7-dicarboxylate, as well as  $S_N$ -Ar reactions. The reduction of ring-fused dimethyl 5,10,15,20-tetrakis(pentafluorophenyl)chlorin-dicarboxylate yielded the corresponding tetrakis(tetrafluorophenyl)chlorin with a diol moiety at the exocyclic pyrazole ring, which proved to be an efficient photosensitizer with  $IC_{50}$  values in the nanomolar range, 72 nM and 56 nM against human melanoma and esophageal carcinoma cell lines, respectively. Combining the diol moiety with short-chained PEG moieties in the same fluorinated ring-fused chlorin led to a molecule with improved balance between photophysics and amphiphilicity, with a singlet oxygen formation quantum yield of 0.45 and high cellular uptake (50% of the initial dose), which make it an even more efficient photosensitizer with  $IC_{50}$  values in the nanomolar range, 13 nM and 27 nM, against human melanoma and esophageal carcinoma cell lines, respectively.

## Experimental

### Chemistry

**General.** Commercially available high-grade materials and reagents were used as received. Organic solvents were

purified by standard procedures prior to utilization.<sup>47</sup> Microwave-assisted reactions were carried out with a CEM Discover S-class focused microwave reactor featuring continuous temperature, pressure and microwave power control, under closed vessel conditions. Reaction monitoring was conducted by TLC analysis, on  $SiO_2$  60 F<sub>254</sub>-coated aluminum plates, and *via* UV-vis absorption spectroscopy, using a PG Instruments T80, Hitachi U-2001 or Shimadzu UV-2100 spectrophotometer. Flash column chromatography was performed using  $SiO_2$  60 (35–70  $\mu$ m) as the stationary phase. Preparative TLC was carried out on  $SiO_2$  60 F<sub>254</sub>-coated glass plates (0.25–0.5 mm, 20  $\times$  20 cm). Melting points were determined with a FALC R132467 electrothermal apparatus, using open glass capillaries, and are uncorrected. NMR spectra were recorded at room temperature with a Bruker Avance III spectrometer, operating at 400 MHz (<sup>1</sup>H) and 376.5 MHz (<sup>19</sup>F). Tetramethylsilane (TMS) was used as an internal standard. Chemical shifts ( $\delta$ ) are expressed in parts per million related to TMS and coupling constants ( $J$ ) are conveyed in hertz. HRMS spectra were obtained with a Waters Micromass VG Autospec M ESI-TOF spectrometer.

**Synthesis of compounds.** 5,10,15,20-Tetrakis(pentafluorophenyl)porphyrin 3<sup>48,49</sup> was prepared based on Lindsey's method for porphyrin synthesis<sup>49–51</sup> and dimethyl 2,2-dioxo-1*H*,3*H*-pyrazolo[1,5-*c*]thiazole-6,7-dicarboxylate 1 was synthesized as described in the literature.<sup>40,41</sup>

**Porphyrin 5.** Microwave heating: a solution of 5,10,15,20-tetrakis(pentafluorophenyl)porphyrin 3 (50 mg, 0.051 mmol) and 2-(2-aminoethoxy)ethanol (10 equiv., 50  $\mu$ L, 0.510 mmol) in NMP (2 mL) was stirred and heated under microwave irradiation at 200  $^{\circ}$ C for 10 min. After cooling to room temperature, the crude product mixture was dissolved in ethyl acetate (50 mL) and washed with a mixture of saturated aqueous  $NaHCO_3$  and NaCl (2  $\times$  50 mL). The organic phase was extracted, dried with anhydrous  $Na_2SO_4$  and evaporated. The resulting residue was purified by flash column chromatography, using ethyl acetate/methanol (9:1) as an eluent. After evaporation of the solvents, tetra-PEGylated porphyrin 5 was obtained as a purple solid in 77% yield (52 mg, 0.039 mmol). Conventional heating: a solution of 5,10,15,20-tetrakis(pentafluorophenyl)porphyrin 3 (500 mg, 0.51 mmol) and 2-(2-aminoethoxy)ethanol (10 equiv., 500  $\mu$ L, 5.10 mmol) in NMP (20 mL) was stirred and heated at 200  $^{\circ}$ C for 3 h. After a similar work-up, porphyrin 5 was isolated in 68% yield (455 mg, 0.346 mmol). MP ( $^{\circ}$ C) >250; <sup>1</sup>H NMR (400 MHz,  $DMSO-d_6$ ):  $\delta$  (ppm) = 9.25 (s, 8H,  $\beta$ -H pyrrolic), 6.43 (s, 4H, NH from PEG), 4.74 (s, 4H, OH from PEG), 3.86–3.72 (m, 16H,  $CH_2$  from PEG), 3.67–3.57 (m, 16H,  $CH_2$  from PEG), –3.09 (s, 2H, NH); <sup>19</sup>F NMR (376.5 MHz,  $DMSO-d_6$ ):  $\delta$  (ppm) = –142.99 (d,  $J = 19.0$  Hz, 8F, Ar-*Ortho*), –160.39 (d,  $J = 19.0$  Hz, 8F, Ar-*Meta*); HRMS (ESI):  $m/z = 1315.3539$  (found), 1315.3569 (calculated for  $C_{60}H_{51}F_{16}N_8O_8$ ,  $[M + H]^+$ ).

**Chlorin 4.** Synthesis of fluorinated ring-fused chlorin 4 was carried out following conventional or microwave heating protocols adapted from a previously described approach for other chlorin derivatives of this type.<sup>23,24</sup> Conventional



heating: a solution of dimethyl 4,6-dihydropyrazolo[1,5-*c*]thiazole-2,3-dicarboxylate **1** (50 mg, 0.182 mmol) and 5,10,15,20-tetrakis(pentafluorophenyl)porphyrin **3** (2 equiv., 350 mg, 0.359 mmol) in 1,2,4-TCB (3 mL) was bubbled with N<sub>2</sub> for 5 min and then stirred and heated at 250 °C for 3 h under an inert atmosphere of N<sub>2</sub>. After cooling to room temperature, 2–3 drops of triethylamine were added to the crude product mixture, and the resulting residue was purified by flash column chromatography, using first dichloromethane as an eluent to recover the unreacted porphyrin and then dichloromethane/ethyl acetate (95:5) to isolate the desired product. After evaporation of the solvents, chlorin **4** was obtained as a purple solid in 28% yield (60 mg, 0.051 mmol). Microwave heating: using the same stoichiometric conditions, the reaction mixture was stirred and heated under microwave irradiation at 250 °C for 20 min. After a similar work-up, chlorin **4** was isolated in 24% yield (51 mg, 0.043 mmol). MP (°C) >250; <sup>1</sup>H NMR (400 MHz, CDCl<sub>3</sub>): δ (ppm) = 8.74 (d, *J* = 5.0 Hz, 1H, overlapping of peaks, β-H pyrrolic), 8.72 (d, *J* = 5.0 Hz, 1H, overlapping of peaks, β-H pyrrolic), 8.49 (s, 2H, β-H pyrrolic), 8.45 (d, *J* = 4.9 Hz, 1H, β-H pyrrolic), 8.35 (d, *J* = 4.9 Hz, 1H, β-H pyrrolic), 5.64–5.57 (m, 1H, reduced β-H pyrrolic), 5.17–5.10 (m, 1H, reduced β-H pyrrolic), 4.65 (dd, *J* = 13.4, 8.0 Hz, 1H, CH<sub>2</sub> from fused ring), 4.22 (dd, *J* = 13.4, 10.0 Hz, 1H, CH<sub>2</sub> from fused ring), 3.95 (s, 3H, CO<sub>2</sub>Me), 3.88 (dd, *J* = 15.5, 6.7 Hz, 1H, CH<sub>2</sub> from fused ring), 3.87 (s, 3H, CO<sub>2</sub>Me), 2.80 (dd, *J* = 15.5, 10.9 Hz, 1H, CH<sub>2</sub> from fused ring), -1.69 (s, 2H, NH); <sup>19</sup>F NMR (376.5 MHz, CDCl<sub>3</sub>): δ (ppm) = -134.61–-134.69 (m, 1F, Ar-*F*<sub>ortho</sub>), -134.86–-134.95 (m, 1F, Ar-*F*<sub>ortho</sub>), -136.79–-136.99 (m, 4F, Ar-*F*<sub>ortho</sub>), -138.11–-138.17 (m, 2F, Ar-*F*<sub>ortho</sub>), -148.72 (t, *J* = 22.6 Hz, 1F, Ar-*F*<sub>para</sub>), -150.75 (t, *J* = 22.6 Hz, 1F, Ar-*F*<sub>para</sub>), -151.35 (t, *J* = 22.6 Hz, 2F, Ar-*F*<sub>para</sub>), -158.00–-158.14 (m, 1F, Ar-*F*<sub>meta</sub>), -158.56–-158.66 (m, 1F, Ar-*F*<sub>meta</sub>), -159.10–-159.22 (m, 1F, Ar-*F*<sub>meta</sub>), -159.75–-159.89 (m, 1F, Ar-*F*<sub>meta</sub>), -161.0–-161.4 (m, 4F, Ar-*F*<sub>meta</sub>); HRMS (ESI): *m/z* = 1185.1302 (found), 1185.1299 (calculated for C<sub>53</sub>H<sub>21</sub>F<sub>20</sub>N<sub>6</sub>O<sub>4</sub>, [M + H]<sup>+</sup>).

**Chlorin 6.** Approach A: a solution of dimethyl 4,6-dihydropyrazolo[1,5-*c*]thiazole-2,3-dicarboxylate **1** (16 mg, 0.058 mmol) and porphyrin **5** (2 equiv., 150 mg; 0.114 mmol) in 1,2,4-TCB (1 mL) was flushed with N<sub>2</sub> for 5 min and then stirred and heated under microwave irradiation at 250 °C for 20 min. After cooling to room temperature, 2–3 drops of triethylamine were added to the crude product mixture, and the resulting residue was purified by flash column chromatography, using ethyl acetate/methanol (9:1) as an eluent. After evaporation of the solvents, chlorin **6** was obtained as a purple solid in 14% yield (12 mg, 0.008 mmol). Approach B: a solution of chlorin **4** (50 mg, 0.042 mmol) and 2-(2-aminoethoxy)ethanol (10 equiv., 42 μL, 0.420 mmol) in 1,4-dioxane (1 mL) was stirred and heated at 50 °C for 192 h. The extent of the reaction was followed by TLC. After cooling to room temperature, the crude product mixture was evaporated, and the resulting residue was purified by flash column chromatography, using first ethyl acetate as an

eluent to remove undesired by-products and then ethyl acetate/methanol (2–10% v/v) to isolate the desired product. A second purification was carried out *via* preparative TLC using ethyl acetate/methanol (95:5) as an eluent. Chlorin **6** was crystallized from diethyl ether and obtained as a purple solid in 12% yield (8 mg, 0.005 mmol). MP (°C) >250; <sup>1</sup>H NMR (400 MHz, CDCl<sub>3</sub>): δ (ppm) = 8.76 (d, *J* = 5.4 Hz, 1H, overlapping of peaks, β-H pyrrolic), 8.74 (d, *J* = 5.4 Hz, 1H, overlapping of peaks, β-H pyrrolic), 8.55 (s, 2H, β-H pyrrolic), 8.46 (d, 1H, *J* = 4.9 Hz, β-H pyrrolic), 8.39 (d, *J* = 4.9 Hz, 1H, β-H pyrrolic), 5.69–5.62 (m, 1H, reduced β-H pyrrolic), 5.14–5.07 (m, 1H, reduced β-H pyrrolic), 4.75 (dd, *J* = 13.3, 8.2 Hz, 1H, CH<sub>2</sub> from fused ring), 4.68 (bs, 4H, NH from PEG), 4.19 (dd, *J* = 13.3, 10.4 Hz, 1H, CH<sub>2</sub> from fused ring), 3.95 (s, 3H, CO<sub>2</sub>Me), 3.91–3.86 (m, 24H, 10xCH<sub>2</sub> from PEG, CH<sub>2</sub> from fused ring and CO<sub>2</sub>Me), 3.77–3.72 (m, 12H, CH<sub>2</sub> from PEG), 2.69 (dd, *J* = 15.8, 11.2 Hz, 1H, CH<sub>2</sub> from fused ring), -1.67 (s, 2H, NH); <sup>19</sup>F NMR (376.5 MHz, CDCl<sub>3</sub>): δ (ppm) = -138.76 (dd, *J* = 23.2, 7.7 Hz, 1F, Ar-*F*<sub>ortho</sub>), -139.14 (dd, *J* = 23.2, 7.7 Hz, 1F, Ar-*F*<sub>ortho</sub>), -140.38–-140.61 (m, 4F, Ar-*F*<sub>ortho</sub>), -141.70 (dd, *J* = 23.2, 7.7 Hz, 1F, Ar-*F*<sub>ortho</sub>), -142.02 (dd, *J* = 23.2, 7.7 Hz, 1F, Ar-*F*<sub>ortho</sub>), -158.17–-159.64 (m, 4F, Ar-*F*<sub>meta</sub>), -160.26–-161.41 (m, 4F, Ar-*F*<sub>meta</sub>); HMRS (ESI): *m/z* = 1525.4164 (found), 1525.4209 (calculated for C<sub>69</sub>H<sub>61</sub>F<sub>16</sub>N<sub>10</sub>O<sub>12</sub>, [M + H]<sup>+</sup>).

**Chlorin 7.** The reduction of the methyl ester substituents of chlorin **4** to dihydroxymethyl groups was performed based on a procedure previously described by us.<sup>26</sup> To a suspension of finely pulverized LiAlH<sub>4</sub> (12 equiv., 18 mg, 0.427 mmol) in dry THF (1.5 mL) at 0 °C was dropwise-added a solution of chlorin **4** (42 mg, 0.036 mmol) in dry THF (1.5 mL). The reaction mixture was allowed to warm to room temperature and left stirring under an inert atmosphere of N<sub>2</sub> for 24 h. It was then cooled with an ice bath and quenched by the addition of ethyl acetate (0.5 mL), followed by water (0.5 mL) and 10% aqueous HCl (0.5 mL). After vigorous stirring at room temperature for 1 h, the crude product mixture was evaporated and the resulting residue was purified by flash column chromatography, using first dichloromethane/ethyl acetate (95:5) as an eluent to remove undesired by-products and then ethyl acetate/methanol (9:1) to isolate the desired product. After evaporation of the solvents, chlorin **7** was obtained as a purple solid in 42% yield (16 mg, 0.015 mmol). MP (°C) >250; <sup>1</sup>H NMR (400 MHz, CDCl<sub>3</sub>): δ (ppm) = 8.72 (d, *J* = 4.9 Hz, 1H, overlapping of peaks, β-H pyrrolic), 8.71 (d, *J* = 4.9 Hz, 1H, overlapping of peaks, β-H pyrrolic), 8.49–8.47 (m, 2H, β-H pyrrolic), 8.43–8.42 (m, 1H, β-H pyrrolic), 8.39–8.38 (m, 1H, β-H pyrrolic), 7.61–7.53 (m, 4H, Ar), 5.60–5.53 (m, 1H, reduced β-H pyrrolic), 5.24–5.17 (m, 1H, reduced β-H pyrrolic), 4.59 (s, 2H, CH<sub>2</sub>OH), 4.46 (dd, *J* = 13.3, 7.6 Hz, 1H, CH<sub>2</sub> from fused ring), 4.37 (s, 2H, CH<sub>2</sub>OH), 4.20 (dd, *J* = 13.3, 9.1 Hz, 1H, CH<sub>2</sub> from fused ring), 3.23 (dd, *J* = 15.3, 6.7 Hz, 1H, CH<sub>2</sub> from fused ring), 2.82 (dd, *J* = 15.3, 9.9 Hz, 1H, CH<sub>2</sub> from fused ring), -1.66–-1.71 (m, 2H, NH tautomerism); <sup>19</sup>F NMR (376.5 MHz, CDCl<sub>3</sub>): δ (ppm) = -135.23–-135.53 (m, 2F), -135.93–-136.39 (m, 3F), -137.29–-137.71 (m, 5F), -138.53–

-138.61 (m, 5F), -139.08--139.11 (m, 1F); HRMS (ESI):  $m/z$  = 1057.1782 (found), 1057.1778 (calculated for  $C_{51}H_{25}F_{16}N_6O_2$ ,  $[M + H]^+$ ).

**Chlorin 8.** The reduction of the methyl ester substituents of chlorin 6 to dihydroxymethyl groups was performed based on a procedure previously described by us.<sup>26</sup> To a suspension of finely pulverized  $LiAlH_4$  (29 equiv., 40 mg, 1.054 mmol) in dry THF (3 mL) at 0 °C was dropwise-added a solution of a mixture (80 mg) bearing chlorin 6 (0.036 mmol) contaminated with porphyrin 5, in a molar ratio of 2:1, respectively, in dry THF (1.5 mL). The reaction mixture was stirred and heated at 50 °C under an inert atmosphere of  $N_2$  for 24 h. It was then cooled with an ice bath and quenched by the addition of ethyl acetate (1 mL), followed by water (1 mL) and 10% aqueous HCl (1.3 mL). After vigorous stirring at room temperature for 2 h, the crude product mixture was evaporated and the resulting residue was purified by flash column chromatography, using ethyl acetate/methanol (8:2) to isolate the desired product. After evaporation of the solvents, chlorin 8 was obtained as a purple solid in 14% yield (7 mg, 0.005 mmol). MP (°C) >250;  $^1H$  NMR (400 MHz,  $CD_4O$ ):  $\delta$  (ppm) = 8.91 (d,  $J$  = 4.2 Hz, 1H, overlapping of peaks,  $\beta$ -H pyrrolic), 8.90 (d,  $J$  = 4.2 Hz, 1H, overlapping of peaks,  $\beta$ -H pyrrolic), 8.64 (d,  $J$  = 4.9 Hz, 1H,  $\beta$ -H pyrrolic), 8.62–8.57 (m, 3H,  $\beta$ -H pyrrolic), 5.61 (dd,  $J$  = 16.5, 8.4 Hz, 1H, reduced  $\beta$ -H pyrrolic), 5.41 (dd,  $J$  = 16.5, 8.4 Hz, 1H, reduced  $\beta$ -H pyrrolic), 4.61–4.56 (m, 1H,  $CH_2$  from fused ring), 4.47–4.40 (m, 2H,  $CH_2OH$ ), 4.37–4.31 (m, 3H,  $CH_2$  from fused ring and  $CH_2OH$ ), 3.89–3.84 (m, 16H,  $CH_2$  from PEG), 3.81–3.77 (m, 10H, 4x $CH_2$  from PEG and 2xNH from PEG), 3.73–3.70 (m, 10H, 4x $CH_2$  from PEG and 2xNH from PEG), 3.43 (dd,  $J$  = 15.2, 7.0 Hz, 1H,  $CH_2$  from fused ring), 3.06 (dd,  $J$  = 15.2, 8.5 Hz, 1H,  $CH_2$  from fused ring);  $^{19}F$  NMR (376.5 MHz,  $CD_4O$ ):  $\delta$  (ppm) = -141.10--141.16 (m, 1F, Ar- $F_{ortho}$ ), -141.25--141.31 (m, 1F, Ar- $F_{ortho}$ ), -144.00--144.15 (m, 4F, Ar- $F_{ortho}$ ), -145.20--145.35 (m, 2F, Ar- $F_{ortho}$ ), -160.89--161.04 (m, 2F, Ar- $F_{meta}$ ), -161.18--161.24 (m, 1F, Ar- $F_{meta}$ ), -161.56--161.62 (m, 1F, Ar- $F_{meta}$ ), -162.55 (d,  $J$  = 9.4 Hz, 4F, Ar- $F_{meta}$ ); HRMS (ESI):  $m/z$  = 735.2183 (found), 735.2192 (calculated for  $C_{67}H_{62}F_{16}N_{10}O_{10}$ ,  $[M + H]^{2+}$ ).

### Photophysics

Solvents were of spectroscopic grade and used as received. Absorption and fluorescence emission spectra were recorded on a Cary 5000 UV-Vis-NIR and Horiba-Jobin-Yvon Fluoromax 4 spectrometer, respectively. All the fluorescence emission spectra were corrected for the wavelength response of the system. Room temperature fluorescence quantum yields were obtained by the comparative method, using *meso*-tetraphenylporphyrin (TPP) in toluene as a reference compound ( $\phi_F$  = 0.11).<sup>52</sup> Fluorescence decays were measured with excitation at 373 nm, using a home-built time correlated single photon counting (TCSPC) apparatus described elsewhere.<sup>53</sup> Deconvolution of the fluorescence decay curves was performed using the modulating function method, as

implemented by G. Striker in the SAND program, as previously reported in the literature.<sup>54</sup> The experimental setup used to obtain the triplet-triplet absorption spectra has been described elsewhere.<sup>55</sup> The samples were irradiated with the third harmonic (355 nm) of a Nd:YAG Spectra Physics laser (Quanta-Ray model). Low laser energy was used to avoid multiphoton and triplet-triplet annihilation effects. The solutions used to collect the transient singlet-triplet difference absorption spectra were bubbled with nitrogen for at least 20 minutes. In general, the obtained transient absorption signals were assigned to the triplet state of the fluorinated chlorins, since first-order kinetics were found and strong quenching was observed in the presence of oxygen. Singlet oxygen quantum yields were determined by direct measurement of the phosphorescence at 1270 nm, followed by the irradiation of the aerated solution of the samples in DMSO with excitation at 355 nm from a Nd:YAG laser with a setup elsewhere described.<sup>53</sup> TPP in toluene was used as a standard ( $\phi_\Delta$  = 0.66).<sup>12</sup> For chlorin 8 the singlet oxygen quantum yield was obtained with a Horiba-Jobin-Yvon SPEX Fluorog 3-2.2 using a NIR Hamamatsu R5509-42 photomultiplier, as previously reported.<sup>53</sup> The sensitized phosphorescence emission spectra of singlet oxygen from optically matched solutions of the samples and that of the reference compound (TPP) were obtained under identical experimental conditions and the singlet oxygen formation quantum yield was determined by comparing the integrated area under the emission spectra of the sample and that of the reference.<sup>53</sup>

### Cell biology

**Cell culture conditions.** The A375 human malignant melanoma cell line was purchased from American Type Culture Collection. The OE19 human esophageal carcinoma cell line was purchased from European Collection of Authenticated Cell Cultures. All cell lines were cultured according to standard procedures at 37 °C, in a humidified incubator with 95% air and 5%  $CO_2$ . The A375 cell line was expanded using Dulbecco's modified Eagle medium (DMEM, Sigma D-5648) supplemented with 10% heat-inactivated fetal bovine serum (FBS, Sigma F7524), 1% penicillin-streptomycin (100 U  $mL^{-1}$  penicillin and 10 mg  $mL^{-1}$  streptomycin, Gibco 15140-122) and 100 mM sodium pyruvate (Gibco Invitrogen Life Technologies; Gibco 1360). The OE19 cell line was propagated using Roswell Park Memorial Institute 1640 medium (RPMI 1640, Sigma R4130) supplemented with 10% heat-inactivated fetal bovine serum (FBS, Sigma F7524), 1% penicillin-streptomycin (100 U  $mL^{-1}$  penicillin and 10 mg  $mL^{-1}$  streptomycin, Gibco 15140-122) and 400 mM sodium pyruvate (Gibco Invitrogen Life Technologies; Gibco 1360). For all studies, cells were detached using a solution of 0.25% trypsin-EDTA (Sigma T4049).

**Photodynamic treatment.** For each experiment, cells were plated and kept in the incubator overnight, to allow the attachment of the cells. The formulation of the sensitizers

consisted of a 1 mg mL<sup>-1</sup> solution in DMSO (Fisher Chemical, 200-664-3) and the desired concentrations being achieved by successive dilutions. The sensitizers were administered in several concentrations (from 1 nM to 10 μM) and cells were incubated for 24 h at 37 °C in the dark. Controls were included on every plate, including untreated cell cultures and cultures treated only with the administration vehicle of the sensitizers, DMSO in a concentration of 1%. Cells were washed with phosphate buffered saline (PBS; in mM: 137 NaCl (JMGs), 2.7 KCl (Sigma), 10 Na<sub>2</sub>HPO<sub>4</sub> (Merck), and 1.8 KH<sub>2</sub>PO<sub>4</sub> (Sigma), pH 7.4) and new drug-free medium was added. Each plate was irradiated with a fluence rate of 7.5 mW cm<sup>-2</sup> until a total of 10 J was reached, using a light source equipped with a red filter (cut off < 560 nm). Evaluation was performed 24 h after the photodynamic treatment.

**Photocytotoxicity and cytotoxicity.** The sensitivity of the cell lines to the sensitizers was analyzed using the MTT colorimetric assay (Sigma M2128; Sigma-Aldrich, Inc.) to measure metabolic activity. Cell culture plates were washed with PBS and incubated, for 4 h at 37 °C in the dark, with a solution of 3-(4,5-dimethylthiazol-2-yl)-2,5-diphenyltetrazolium bromide (0.5 mg mL<sup>-1</sup>, Sigma M5655) in PBS (pH 7.4). To solubilize formazan crystals, a 0.04 M solution of hydrochloric acid (Merck Millipore 100317) in isopropanol (Sigma 278475) was added. Absorbance was measured using an EnSpire Multimode Plate Reader (PerkinElmer). Cytotoxicity was expressed as the percentage relative to cell cultures treated only with the administration vehicle of the sensitizers. Dose–response curves were obtained using Prism 9.0 and the concentration of sensitizers that inhibits the proliferation of cultures in 50% (IC<sub>50</sub>) was derived. Dark cytotoxicity studies were performed as described above, but omitting the irradiation step.

**Cell uptake.** Cells (5 × 10<sup>5</sup>) were incubated with the sensitizers in concentrations of 500 nM for 24 h in the dark. Cells were then washed with PBS and disrupted with DMSO. Cell scrappers were used to ensure full disaggregation. The solutions were collected and centrifuged, with the fluorescence intensity of the supernatants being determined by fluorescence emission spectroscopy with an EnSpire Multimode Plate Reader (Perkin Elmer), using 405 and 420 nm as excitation wavelengths. The intracellular concentration was determined using a calibration curve obtained from the fluorescence intensity in DMSO solutions for each sensitizer.

## Conflicts of interest

The authors declare no personal, professional or financial conflicts of interest.

## Acknowledgements

The authors thank Coimbra Chemistry Centre (CQC), supported by the Portuguese Agency for Scientific Research, “Fundação para a Ciência e a Tecnologia” (FCT) through

project UIDB/00313/2020 and UIDP/QUI/00313/2020, co-funded by COMPETE2020-UE. Center for Innovative Biomedicine and Biotechnology (CIBB) is funded by FCT (UID/NEU/04539/2013) and COMPETE-FEDER (POCI-01-0145-FEDER-007440), through the Strategic Project UIDB/04539/2020 and UIDP/04539/2020. Thanks are also due to CIMAGO (Project 06/2019) and FCT, co-funded by the European Regional Development Fund (FEDER) through Portugal 2020/CENTRO 2020 (CENTRO-01-0145-FEDER-000014/MATIS). João Braz thanks FCT/CQC for the PhD scholarship UI/BD/150880/2021. The authors also acknowledge the UC-NMR facility for obtaining the NMR data (www.nmrcc.uc.pt).

## References

- 1 H. Abrahamse and M. R. Hamblin, New photosensitizers for photodynamic therapy, *Biochem. J.*, 2016, **473**, 347–364.
- 2 M. R. Hamblin, Antimicrobial photodynamic inactivation: a bright new technique to kill resistant microbes, *Curr. Opin. Microbiol.*, 2016, **33**, 67–73.
- 3 D. Dolmans, D. Fukumura and R. N. K. Jain, Photodynamic therapy for cancer, *Nat. Rev. Cancer*, 2003, **3**, 380–387.
- 4 K. Plaetzer, B. Krammer, J. Berlanda, F. Berr and T. Kiesslich, Photophysics and photochemistry of photodynamic therapy: fundamental aspects, *Lasers Med. Sci.*, 2009, **24**, 259–268.
- 5 S. B. Brown, E. A. Brown and I. Walker, The present and future role of photodynamic therapy in cancer treatment, *Lancet Oncol.*, 2004, **5**, 497–508.
- 6 C. Hopper, Photodynamic therapy: a clinical reality in the treatment of cancer, *Lancet Oncol.*, 2000, **1**, 212–219.
- 7 D. van Straten, V. Mashayekhi, H. S. de Bruijn, S. Oliveira and D. J. Robinson, Oncologic photodynamic therapy: basic principles, current clinical status and future directions, *Cancers*, 2017, **9**, 19.
- 8 D. Luo, K. A. Carter, D. Miranda and J. F. Lovell, Chemophototherapy: an emerging treatment option for solid tumors, *Adv. Sci.*, 2017, **4**, 1600106.
- 9 J. M. Dabrowski and L. G. Arnaut, Photodynamic therapy (PDT) of cancer: from local to systemic treatment, *Photochem. Photobiol. Sci.*, 2015, **14**, 1765–1780.
- 10 S. O. Gollnick and C. M. Brackett, Enhancement of anti-tumor immunity by photodynamic therapy, *Immunol. Res.*, 2010, **46**, 216–226.
- 11 F. Bray, J. Ferlay, I. Soerjomataram, R. L. Siegel, L. A. Torre and A. Jemal, Global cancer statistics 2018: GLOBOCAN estimates of incidence and mortality worldwide for 36 cancers in 185 countries, *Ca-Cancer J. Clin.*, 2018, **68**, 394–424.
- 12 M. Pineiro, A. L. Carvalho, M. M. Pereira, A. M. d'A. R. Gonsalves, L. G. Arnaut and S. J. Formosinho, Photoacoustic Measurements of Porphyrin Triplet-State Quantum Yields and Singlet-Oxygen Efficiencies, *Chem. – Eur. J.*, 1998, **4**, 2299–2307.
- 13 S. Anand, B. J. Ortel, S. P. Pereira, T. Hasan and E. V. Maytin, Biomodulatory approaches to photodynamic therapy for solid tumors, *Cancer Lett.*, 2012, **326**, 8–16.

- 14 M. L. Davila, Photodynamic Therapy, *Gastrointest. Endosc. Clin. N. Am.*, 2011, **21**, 67–79.
- 15 W. H. Allum, J. M. Blazeby, S. M. Griffin, D. Cunningham, J. A. Jankowski and R. Wong, Guidelines for the management of oesophageal and gastric cancer, *Gut*, 2011, **60**, 1449–1472.
- 16 T. Yano, M. Muto, K. Yoshimura, M. Niimi, Y. Ezoe, Y. Yoda, Y. Yamamoto, H. Nishisaki, K. Higashino and H. Iishi, Phase I study of photodynamic therapy using talaporfin sodium and diode laser for local failure after chemoradiotherapy for esophageal cancer, *Radiat. Oncol.*, 2012, **7**, 113.
- 17 K. Kalka, H. Merk and H. Mukhtar, Photodynamic therapy in dermatology, *J. Am. Acad. Dermatol.*, 2000, **42**, 389–413.
- 18 Y.-Y. Huang, D. Vecchio, P. Avci, R. Yin, M. Garcia-Diaz and M. R. Hamblin, Melanoma resistance to photodynamic therapy: new insights, *Biol. Chem.*, 2013, **394**, 239–250.
- 19 S. Swavey and M. Tran, Porphyrin and Phthalocyanine Photosensitizers as PDT Agents: A New Modality for the Treatment of Melanoma, in *Recent Advances in the Biology, Therapy and Management of Melanoma*, ed. L. Davids, IntechOpen, London, UK, 2013, pp. 253–282.
- 20 L. R. Milgrom, *The colours of life: an introduction to the chemistry of porphyrins and related compounds*, Oxford University Press, Oxford, UK, 1997.
- 21 T. W. Liu, E. Huynh, T. D. MacDonald and G. Zheng, Porphyrins for imaging, photodynamic therapy, and photothermal therapy, in *Cancer Theranostics*, ed. X. Chen and S. Wong, Academic Press, Oxford, UK, 2014, pp. 229–254.
- 22 J. P. Celli, B. Q. Spring, I. Rizvi, C. L. Evans, K. S. Samkoe, S. Verma, B. W. Pogue and T. Hasan, Imaging and photodynamic therapy: mechanisms, monitoring and optimization, *Chem. Rev.*, 2010, **110**, 2795–2838.
- 23 N. A. M. Pereira, A. C. Serra and T. M. V. D. Pinho e Melo, Novel approach to chlorins and bacteriochlorins:  $[8\pi+2\pi]$  cycloaddition of diazafulvenium methides with porphyrins, *Eur. J. Org. Chem.*, 2010, 6539–6543.
- 24 N. A. M. Pereira, S. M. Fonseca, A. C. Serra, T. M. V. D. Pinho e Melo and H. D. Burrows,  $[8\pi+2\pi]$  Cycloaddition of meso-tetra- and 5,15-diarylporphyrins: synthesis and photophysical characterization of stable chlorins and bacteriochlorins, *Eur. J. Org. Chem.*, 2011, 3970–3979.
- 25 N. A. M. Pereira, M. Laranjo, M. Pineiro, A. C. Serra, K. Santos, R. Teixo, A. M. Abrantes, A. C. Goncalves, A. B. Sarmiento Ribeiro, J. Casalta-Lopes, M. Filomena Botelho and T. M. V. D. Pinho e Melo, Novel 4,5,6,7-tetrahydropyrazolo[1,5-a] pyridine fused chlorins as very active photodynamic agents for melanoma cells, *Eur. J. Med. Chem.*, 2015, **103**, 374–380.
- 26 N. A. M. Pereira, M. Laranjo, J. Pina, A. S. R. Oliveira, J. D. Ferreira, C. Sanchez-Sanchez, J. Casalta-Lopes, A. C. Goncalves, A. B. Sarmiento-Ribeiro, M. Pineiro, J. S. Seixas de Melo, M. F. Botelho and T. M. V. D. Pinho e Melo, Advances on photodynamic therapy of melanoma through novel ring-fused 5,15-diphenylchlorins, *Eur. J. Med. Chem.*, 2018, **146**, 395–408.
- 27 B. F. O. Nascimento, M. Laranjo, N. A. M. Pereira, J. Dias-Ferreira, M. Pineiro, M. F. Botelho and T. M. V. D. Pinho e Melo, Ring-Fused Diphenylchlorins as Potent Photosensitizers for Photodynamic Therapy Applications: In Vitro Tumor Cell Biology and in Vivo Chick Embryo Chorioallantoic Membrane Studies, *ACS Omega*, 2019, **4**, 17244–17250.
- 28 N. A. M. Pereira, M. Laranjo, J. Casalta-Lopes, A. C. Serra, M. Pineiro, J. Pina, J. S. Seixas de Melo, M. O. Senge, M. Filomena Botelho, L. Martelo, H. D. Burrows and T. M. V. D. Pinho e Melo, Platinum(II) ring-fused chlorins as near-infrared emitting oxygen sensors and photodynamic agents, *ACS Med. Chem. Lett.*, 2017, **8**, 310–315.
- 29 M. Laranjo, M. C. Aguiar, N. A. M. Pereira, G. Brites, B. F. O. Nascimento, A. F. Brito, J. Casalta-Lopes, A. C. Gonçalves, A. B. Sarmiento-Ribeiro, M. Pineiro, M. F. Botelho and T. M. V. D. Pinho e Melo, Platinum(II) ring-fused chlorins as efficient theranostic agents: Dyes for tumor-imaging and photodynamic therapy of cancer, *Eur. J. Med. Chem.*, 2020, **200**, 112468.
- 30 D. Samaroo, M. Vinodu, X. Chen and C. M. Drain, meso-Tetra(pentafluorophenyl)porphyrin as an Efficient Platform for Combinatorial Synthesis and the Selection of New Photodynamic Therapeutics using a Cancer Cell Line, *J. Comb. Chem.*, 2007, **9**, 998–1011.
- 31 S. Tsuchiya, Intramolecular Electron Transfer of Diporphyrins Comprised of Electron-Deficient Porphyrin and Electron-Rich Porphyrin with Photocontrolled Isomerization, *J. Am. Chem. Soc.*, 1999, **121**, 48–53.
- 32 S. Tsuchiya and M. Seno, Novel Synthetic Method of Phenol from benzene Catalysed by perfluorinated Hemin, *Chem. Lett.*, 1989, 263–266.
- 33 J. C. P. Grancho, M. M. Pereira, M. G. Miguel, A. M. d'A. Rocha Gonsalves and H. D. Burrows, Synthesis, Spectra and Photophysics of some Free Base Tetrafluoroalkyl and Tetrafluoroaryl Porphyrins with Potential Applications in Imaging, *Photochem. Photobiol.*, 2002, **75**, 249–256.
- 34 L. Benov, Photodynamic therapy: current status and future directions, *Med. Princ. Pract.*, 2015, **24**, 14–28.
- 35 A. P. Castano, T. N. Demidova and M. R. Hamblin, Mechanisms in photodynamic therapy: Part three - Photosensitizer pharmacokinetics, biodistribution, tumor localization and modes of tumor destruction, *Photodiagn. Photodyn. Ther.*, 2005, **2**, 91–106.
- 36 M. Luciano and C. Brückner, Modifications of porphyrins and hydroporphyrins for their solubilization in aqueous media, *Molecules*, 2017, **22**, 980.
- 37 J. I. T. Costa, A. C. Tomé, M. G. P. M. S. Neves and J. A. S. Cavaleiro, 5,10,15,20-tetrakis(pentafluorophenyl)porphyrin: a versatile platform to novel porphyrinic materials, *J. Porphyrins Phthalocyanines*, 2011, **15**, 1116–1133.
- 38 D. Samaroo, C. E. Soll, L. J. Todaro and C. M. Drain, Efficient microwave-assisted synthesis of amine-substituted tetrakis(pentafluorophenyl)porphyrin, *Org. Lett.*, 2006, **8**, 4985–4988.
- 39 B. H. Song and B. S. Yu, Fluorine-19 NMR spectroscopic studies of phenyl-fluorinated iron tetraarylporphyrin complexes, *Bull. Korean Chem. Soc.*, 2003, **24**, 981–985.

- 40 O. B. Sutcliffe, R. C. Storr, T. L. Gilchrist and P. Rafferty, Azafulvenium methides: new extended dipolar systems, *J. Chem. Soc., Perkin Trans. 1*, 2001, 1795–1806.
- 41 O. B. Sutcliffe, R. C. Storr, T. L. Gilchrist, P. Rafferty and A. P. A. Crew, Azafulvenium methides: new extended dipolar systems, *Chem. Commun.*, 2000, 675–676.
- 42 S.-K. Chung and F.-f. Chung, Reduction of aryl bromides with lithium aluminum hydride: Evidence for a radical mechanism, *Tetrahedron Lett.*, 1979, **20**, 2473–2476.
- 43 J. A. Hendrix and D. W. Stefany, A mild chemospecific reductive dehalogenation of ethylaminobenzamides with lithium aluminum hydride, *Tetrahedron Lett.*, 1999, **40**, 6749–6752.
- 44 G. J. Karabatsos and R. L. Shone, Reaction of lithium aluminum hydride with aromatic halides, *J. Org. Chem.*, 1968, **33**, 619–621.
- 45 J. N. Silva, A. M. G. Silva, J. P. Tomé, A. O. Ribeiro, M. R. M. Domingues, J. A. S. Cavaleiro, A. M. S. Silva, M. G. P. M. S. Neves, A. C. Tomé, O. A. Serra, F. Bosca, P. Filipe, R. Santus and P. Morlière, Photophysical properties of a photocytotoxic fluorinated chlorin conjugated to four  $\beta$ -cyclodextrins, *Photochem. Photobiol. Sci.*, 2008, **7**, 834–843.
- 46 J. A. S. Cavaleiro, H. Görner, P. S. S. Lacerda, J. G. MacDonalde, G. Mark, M. G. P. M. S. Neves, R. S. Nohr, H.-P. Schuchmann, C. von Sonntag and A. C. Tomé, Singlet oxygen formation and photostability of meso-tetraarylporphyrin derivatives and their copper complexes, *J. Photochem. Photobiol., A*, 2001, **144**, 131–140.
- 47 W. L. F. Armarego and D. D. Perrin, *Purification of Laboratory Chemicals*, Butterworth-Heinemann, 4th edn, 1997.
- 48 M. A. Carvalho de Medeiros, S. Cosnier, A. Deronzier and J.-C. Moutet, Synthesis and Characterization of a New Series of Nickel(II) meso-Tetrakis (polyfluorophenyl)porphyrins Functionalized by Pyrrole Groups and Their Electropolymerized Films, *Inorg. Chem.*, 1996, **35**, 2659–2664.
- 49 J. S. Lindsey and R. W. Wagner, Investigation of the synthesis of ortho-substituted tetraphenylporphyrins, *J. Org. Chem.*, 1989, **54**, 828–836.
- 50 J. S. Lindsey, H. C. Hsu and I. C. Schreiman, Synthesis of tetraphenylporphyrins under very mild conditions, *Tetrahedron Lett.*, 1986, **27**, 4969–4970.
- 51 J. S. Lindsey, I. C. Schreiman, H. C. Hsu, P. C. Kearney and A. M. Marguerettaz, Rothmund and Adler-Longo reactions revisited: synthesis of tetraphenylporphyrins under equilibrium conditions, *J. Org. Chem.*, 1987, **52**, 827–836.
- 52 M. Montalti, A. Credi, L. Prodi and M. T. Gandolfi, *Handbook of Photochemistry*, CRC Press, 3rd edn, 2006.
- 53 J. S. Seixas de Melo, J. Pina, F. B. Dias and A. L. Maçanita, Experimental Techniques for Excited State Characterization, in *Applied Photochemistry*, ed. R. C. Evans, P. Douglas and H. D. Burrows, Springer, 2013, pp. 533–585.
- 54 G. Striker, V. Subramaniam, C. A. M. Seidel and A. Volkmer, Photochromicity and Fluorescence Lifetimes of Green Fluorescent Protein, *J. Phys. Chem. B*, 1999, **103**, 8612–8617.
- 55 J. Pina, J. Seixas de Melo, H. D. Burrows, A. Bilge, T. Farrell, M. Forster and U. Scherf, Spectral and Photophysical Studies on Cruciform Oligothiophenes in Solution and the Solid State, *J. Phys. Chem. B*, 2006, **110**, 15100–15106.